Journal of Controlled Release 263 (2017) 4–17

Contents lists available at ScienceDirect

Journal of Controlled Release

journal homepage: www.elsevier.com/locate/jconrel

Rational design of polyarginine nanocapsules intended to help peptides overcoming intestinal barriers

Zhigao Niu [a], Erik Tedesco [b], Federico Benetti [b], Aloïse Mabondzo [c], Isabella Monia Montagner [d], Ilaria Marigo [d], David Gonzalez-Touceda [e], Sulay Tovar [e], Carlos Diéguez [e], Manuel J. Santander-Ortega [a,f], María J. Alonso [a,*]

[a] Department of Pharmacy and Pharmaceutical Technology, CIMUS Research Institute, IDIS research Institute, University of Santiago de Compostela, 15782 Santiago de Compostela, Spain
[b] ECSIN-European Center for the Sustainable Impact of Nanotechnology, ECAMRICERT SRL, I-45100 Rovigo, Italy
[c] Service de Pharmacologie et d'Immunoanalyse, IBITECS, CEA, Université Paris-Saclay, F-91191 Gif-sur-Yvette, France
[d] Veneto Institute of Oncology, IOV-IRCCS, 35128 Padova, Italy
[e] Biomedical Research Group, Center for Research in Molecular Medicine and Chronic Diseases, University of Santiago de Compostela, 15782 Santiago de Compostela, Spain
[f] Cellular Neurobiology and Molecular Chemistry of the Central Nervous System Group, Universidad de Castilla-La Mancha, Spain

ARTICLE INFO

Article history:
Received 7 December 2016
Received in revised form 2 February 2017
Accepted 19 February 2017
Available online 21 February 2017

Keywords:
Polyarginine
Nanocapsule
Insulin
Permeation enhancer
Oral peptide delivery

ABSTRACT

The aim of this work was to rationally design and characterize nanocapsules (NCs) composed of an oily core and a polyarginine (PARG) shell, intended for oral peptide delivery. The cationic polyaminoacid, PARG, and the oily core components were selected based on their penetration enhancing properties. Insulin was adopted as a model peptide to assess the performance of the NCs. After screening numerous formulation variables, including different oils and surfactants, we defined a composition consisting of oleic acid, sodium deoxycholate (SDC) and Span 80. This selected NCs composition, produced by the solvent displacement technique, exhibited the following key features: (i) an average size of 180 nm and a low polydispersity (0.1), (ii) a high insulin association efficacy (80–90% AE), (iii) a good colloidal stability upon incubation in simulated intestinal fluids (SIF, FaSSIF-V2, FeSSIF-V2), and (iv) the capacity to control the release of the associated insulin for >4 h. Furthermore, using the Caco-2 model cell line, PARG nanocapsules were able to interact with the enterocytes, and reversibly modify the TEER of the monolayer. Both cell adhesion and membrane permeabilization could account for the pronounced transport of the NCs-associated insulin (3.54%). This improved interaction was also visualized by confocal fluorescent microscopy following oral administration of PARG nanocapsulesto mice. Finally, *in vivo* efficacy studies performed in normoglycemic rats showed a significant decrease in their plasma glucose levels after treatment. In conclusion, here we disclose key formulation elements for making possible the oral administration of peptides.

1. Introduction

Peptide therapeutics has drawn increasing interest in the pharmaceutical market since the 1970s. Over the last decades, the regulatory approval rate of these products has been shown to be superior to that of small molecules, and their global value has increased from 14.1 to 25.4 billion USD from 2011 to 2018 [1]. Currently, over 500 peptide drugs are under preclinical development, 140 are candidates in clinical trials and about 60 commercialized products have been approved by the FDA [2]. Due to their complex structure, these macromolecules offer high specificity, advanced drug potency, low toxicity and less interaction with other drugs when compared to small molecules. However, because of their physicochemical properties, their delivery to the subjects' body represents a critical challenge. In particular, these macromolecules are prone to lose their activity in a physiological environment and have great difficulties to cross biological barriers. Because of this, up to date, peptide therapeutics is principally administrated *via* injection, which is an easy but inconvenient way of medication.

Oral administration is the most attractive modality for the administration of peptide drugs. However, peptides administered by this route would have to overcome major barriers, including the harsh gastrointestinal environment, the mucus layer and the underlying epithelium barrier [3]. The approaches investigated so far to improve the intestinal absorption of peptides include the chemical modification of the peptide molecule, the co-administration of protease inhibitors and/or permeation enhancers, and the incorporation of the peptide formulation to delivery carriers [4,5]. A broad array of carriers including polymeric micro and nanoparticles, silica nanoparticles, liposomes, micelles, solid lipid nanoparticles, microemulsions, self-emulsifying drug delivery systems, nanoemulsions and NCs have been explored for the delivery of peptide drugs [6–8]. Among them, liver-targeted HDV-I liposomes of specific composition [9], bioadhesive calcium phosphate nanoparticles in an enteric capsule [10], and silica nanoparticles [11] have reached the clinical

* Corresponding author.
E-mail address: mariajalonso@usc.es (M.J. Alonso).

http://dx.doi.org/10.1016/j.jconrel.2017.02.024

development phase for the delivery of insulin. Although the basis for the success of these delivery carriers has not been described in detail, it is generally assumed that these carriers have the capacity to overcome the GI barriers.

Within this frame, our laboratory has contributed with the design of NCs consisting of an oily core surrounded by a shell made of chitosan [12–15]. These NCs allowed us to encapsulate the peptide salmon calcitonin (sCT), and the resulting nanocomposition was found to facilitate and prolong sCT absorption following oral administration. More recently, we have also explored the interaction of PARG nanocapsules based on Miglyol® core [16] with the Caco-2 monolayer [17] and concluded that PARG NC may have a potential for oral delivery. Taking into account this background information, the objective of this work was to engineer a new composition based on PARG NCs that would endow them with the capacity to load peptides, *i.e.* insulin, and to overcome the biological barriers associated with the oral modality of administration. Hence, the main criteria for this design were: i) efficient encapsulation and controlled release of the selected peptide, *i.e.* insulin; ii) stability in the intestinal fluids, in the presence of enzymes and bile salts; iii) capacity to diffuse across the mucus layer and, iv) capacity to interact with the intestinal epithelium and facilitate the transport of the associated peptide across it. With these criteria in mind, we performed a thoughtful analysis of the potential ingredients to form the lipid core, and selected oleic acid and SDC because of their permeation enhancing properties [18–22]. Besides, SDC is known to form complexes with insulin during the formulation process, thus improving the encapsulation of insulin [23,24]. On the other hand, we chose polyarginine (PARG) as the material to form the polymer shell. Finally, to facilitate the dispersion of the oily droplets and improve the stability of the NCs in the intestinal fluids, we selected surfactants with different HLB values, *i.e.* poloxamer 188 and Span®80 [25]. Once formulated, we determined the physicochemical properties of these NCs and their capacity to promote the absorption of insulin in different *in vitro* and *in vivo* intestinal models.

2. Materials and methodology

2.1. Materials

Recombinant human insulin hexamer Insuman® (Mw 5808 Da) was kindly provided by Sanofi (Paris, France). Poly-L-Arginine (Mw 26–37 kDa) was purchased from Polypeptide Therapeutic Solutions (PTS, Valencia, Spain). Analytical grade poloxamer 188, oleic acid, Span® 80, SDC and Triton™ X-100 were purchased from Sigma Aldrich (St. Louis, USA). Pharmaceutical grade poloxamer 188 was purchased from BASF (Ludwigshafen, Germany); pharmaceutical grade oleic acid and Span® 80 were purchased from Croda (Snaith, UK); pharmaceutical grade SDC was purchased from New Zealand Pharmaceuticals (Palmerston North, New Zealand). Pancreatin (8xUSP) was purchased from Biozym (Hamburg, Germany). Sephadex® G-50 was purchased from GE healthcare (Little Chalfont, UK). The 1,10-dioctadecyl-3,3,30,30-tetramethylindodicarbocyanine perchlorate fluorescent dye (DiD oil, Em 644 nm; Ex 663 nm) was obtained from Life Technologies (Eugene, USA). Human colorectal adenocarcinoma Caco-2 cells (ATCC® HTB37 ™) were purchased from American Type Culture Collection (Manassas, VA, USA). High glucose Dulbecco's modified eagle medium (DMEM) and non-essential amino acid (NEAA) solution were purchased from Sigma Aldrich (St. Louis, USA), while heat inactivated fetal bovine serum (FBS), penicillin-streptomycin solution, L-glutamine, phosphate-buffered saline (PBS), Dulbecco's phosphate-buffered saline with calcium and magnesium (DPBS) were purchased from Lonza (Basel, Switzerland). Reagents for cytotoxicity assays were MTS based CellTiter 96® AQueous Non-Radioactive Cell Proliferation Assay kit (Promega, Madison, USA), LDH cytotoxicity detection kit plus (Roche, Mannheim, Germany) and Neutral Red based *In Vitro* Toxicology Assay Kit, (Sigma Aldrich, St. Louis, USA). Ultrapurified water was obtained from Millipore Milli-Q Plus water purification system (Darmstadt, Germany). HCl and NaOH solutions are purchased from Scharlab (Barcelona, Spain). All the other chemicals were of analytical grade.

2.2. Preparation of the PARG NCs

Polyarginine based NCs were prepared by a modified solvent displacement technique previously developed by our laboratory [26,27]. Different oils (oleic acid or Miglyol® 812N) and surfactants (Span®80, Tween®80 or Labrasol®) at different concentrations were explored for the formation of the NC's core. Finally, at the optimum condition, insulin was dissolved in 0.01 N HCl (pH ~ 2.1) at a concentration of 15 mg/mL, and 0.1 mL of this solution was transferred to an organic phase composed by 62.5 μL oleic acid, 20 mg surfactant Span®80, 4.1 mL acetone and 0.8 mL ethanol with/without 2.5 mg SDC. This organic phase was mixed using a vortex agitator (VELP Scientifica, Usmate, Italy) and immediately poured onto 10 mL of ultrapure water or pH 5.5 acetate/citrate buffer. In the first case, the pH of the external aqueous phase was adjusted with 0.1 N NaOH. Alternatively, 10 mM, 20 mM, 30 mM and 50 mM pH 5.5 acetate or citrate buffer was used to prepare the aqueous phase to ensure the desired final formulation pH (pH 5.5). In all cases, the aqueous phase solution contained 0.05% (w/v) PARG and 0.25% (w/v) of poloxamer 188. After magnetic stirring for 10 min, the solvents were evaporated under vacuum, decreasing the volume of the final formulation from 15 mL to 5 mL in a rotavapor (Heidolph Hei-VAP Advantage, Schwabach, Germany). Oleic acid-based nanoemulsions, used as controls for some experiments, were prepared by the same method without incorporating PARG.

Fluorescent NCs to be used for *in vitro*/*in vivo* studies were also produced by adding 50 μg DiD to the organic phase. The absence of dye leakage was assessed upon incubation of the nanocapsules in PBS, at 37 °C for up to 4 h.

2.3. Physicochemical and morphological characterization of PARG NCs

Particle size distribution and PDI were determined by dynamic light scattering (DLS) and zeta potential was calculated from the electrophoretic mobility values determined by laser doppler anemometry (LDA). Both were obtained with a Malvern Zeta-sizer device (NanoZS, ZEN 3600, Malvern Instruments, Worcestershire, UK) equipped with a red laser light beam ($\lambda = 632.8$ nm). To measure the particle size and PDI, a volume of 50 μL of the formulations was diluted with 950 μL of ultrapure water. For the *Z*-potential measurements, the sample was diluted with 1 mM KCl solution in the same proportion. The analysis was performed at 25 °C with at least, three different batches and each batch was analyzed in triplicate. The morphological analysis of the NCs was carried out in a transmission electron microscope (TEM, CM12, Philips, Netherlands). The samples were stained with phosphotungstic acid (2%, w/v) solution and placed on cupper grids with Formvard® for TEM observation.

2.4. Association of insulin to PARG NCs

The AE of insulin to PARG NCs was determined upon separation of the NCs from the suspending aqueous medium. The analysis was done by both indirect and direct methods. Briefly, in the indirect method, 2 mL of NC formulation was ultracentrifuged (Beckman Coulter, Optima L-90K, Brea, USA) at 82,656 g for 1 h at 15 °C, and the amount of free insulin in the undernatant was determined using reverse phase isocratic HPLC (Agilent, 1100 Series, Santa Clara, USA) method. The phosphoric acid/sodium perchlorate buffer was mixed with acetonitrile at different volume phase ratios, in order to produce two different mobile phases (93:7 as phase A and 43:57 as phase B), and C18 column (Superspher® RP-18 endcapped) was used as stationary phase. The AE of insulin in

NCs was calculated according to the equation:

$$AE(\%) = \frac{Total\ insulin - Free\ insulin}{Total\ insulin} X100$$

where *Total insulin* is the theoretical total insulin concentration in the formulation, and *Free insulin* is the insulin concentration determined by HPLC. Analysis was done in triplicate.

When using the direct method, 500 μL of NCs were isolated from the suspension medium by size exclusion chromatography using Sephadex-G50 column. The cream fractions and the transparent aqueous fractions were collected in microtubes. Insulin was extracted from the NC cream following the next steps: 1) 100 μL of the cream were vortexed with 100 μL of acetonitrile for 2 min, 2) 100 μL of Triton™ X-100 were added to the previous mixture and vortexed for 2 min, 3) 700 μL of 0.1% (v/v) of a trifluoroacetic acid (TFA) solution were added to the mixture and all the components were vortexed. Finally, both the broken NCs and the transparent aqueous fractions were analyzed by HPLC in order to determine the amount of insulin associated to the NCs and also in the suspending medium. Simultaneously, 500 μL of non-isolated NCs were degraded following the same procedure and the total insulin concentration was determined by HPLC, by which the gross mass of insulin in 500 μL NC formulation was obtained. The AE of insulin in NCs was calculated dividing the amount determined in the isolated NC cream by the amount determined in the non-isolated NCs. Analysis was done in triplicate.

The final insulin loading (% w/w) was calculated by dividing the amount of insulin associated (AE × *Total Insulin* in the formulation) by the total weight of the NCs. For the calculation of the total weight of the NCs, 500 μL of the formulation were isolated by ultrafiltration using 100k Amicon® filters (Merck Millipore, Carrigtwohill, Ireland), a method that facilitates the re-suspension of NCs without diluting the sample. The NC cream was resuspended to 500 μL and lyophilized solely in microtubes, which were weighed before adding NC sample and after freeze drying to assess the solid mass of the cream. The yield of PARG NCs was calculated by a division of isolated and non-isolated NCs cream weight after freeze-drying.

2.5. Stability of PARG NCs in simulated intestinal media

The colloidal stability of NCs in simulated intestinal fluids was evaluated by analysis of the particle size and PDI by DLS. Additionally, particle concentration of the sample was monitored by analysis of the light intensity count rate. To mimic the intestinal environment following oral delivery, SIF, FaSSIF-V2 (pH 6.5) and FeSSIF-V2, (pH 5.8) were prepared (for composition, see supplementary material on Table 1). FaSSIF-V2 and FeSSIF-V2 are updated versions of the FaSSIF and FeSSIF media described in the pharmacopeia, to better mimic the *in vivo* fasted and fed state intestinal conditions [28,29]. The study was carried out using 50 μL of NCs that were diluted in 950 μL of simulated intestinal media in a microtube, and then placed in an incubator at 37 °C (Heidolph Instruments GmbH & Co. KG, Schwabach, Germany) with a horizontal shaking at speed 300 rpm. At different time points (0 h, 0.5 h, 1 h, 2 h and 4 h), 50 μL samples were withdrawn and the particle size, PDI, and count rate were determined at the different time points using Malvern Zeta-sizer (Attenuator 6). To exclude the interference of pancreatin aggregates in particle size measurements, after incubation of NCs in FeSSIF-V2, the microtubes were centrifuged at 13,600 g for 5 min, so the pancreatin precipitated and was isolated from the suspension media. Each analysis was performed by triplicate in three different batches. The colloidal stability of the NCs under storage condition was analyzed as follows: different aliquots of the formulation were conserved at room temperature (around 20 °C). The particle size, PDI and count rate were monitored up to 45 days to check the potential destabilization of the formulation. The insulin remaining in the formulation was also determined.

2.6. In vitro release profile of insulin from PARG NCs

The amount of insulin released *in vitro* upon incubation of PARG NCs in SIF and FaSSIF-V2 media, at 37 °C under horizontal shaking (300 rpm) was quantified by HPLC. Specifically, aliquots of 0.25 mL of insulin-loaded NCs were diluted with 1.25 mL of the desired intestinal media and placed in an incubator. After 0, 2, 3, 3.5 and 4 h, samples were withdrawn and ultracentrifuged (82,656 g; 4 °C; 1 h). The amount of free insulin and insulin associated to the NCs was evaluated by HPLC upon treatment with Triton™ X-100, acetonitrile and 0.1% TFA (same method as the one described in Section 2.4).

2.7. Caco-2 cells culture

Caco-2 cells were grown in DMEM high glucose with L-glutamine supplemented with 10% heat inactivated fetal bovine serum, 1% Penicillin (100 U/mL), streptomycin (100 μg/mL), and 1% NEAA solution. Cells were maintained at 37 °C in a humidified incubator supplied with 5% CO_2.

2.8. Toxicity studies on Caco-2 cells

For cytotoxicity evaluation, Caco-2 cells were seeded in 96-well plates at the density of 10,000 viable cells/well, and incubated for 24 h to allow the cell attachment. Cells were then incubated with increasing concentrations of the tested samples, whose colloidal stability of NCs in cell culture medium has been confirmed in advance. The cytotoxicity of PARG NCs was determined by measuring the metabolic activity with neutral red uptake (NRU). Lactate dehydrogenase (LDH)-based cytotoxicity assay was also used to measure LDH released into media from damaged cells as a biomarker for cellular cytotoxicity and cytolysis. In the study, the cell culture medium was replaced by the PARG NC (or nanoemulsion) suspension in cell culture medium at concentration 0.1855, 0.371, 0.742, 1.484, 2.968, 4.452, and 5.936 mg/mL. The plate of Caco-2 monolayers was transferred to a humid incubator at 37 °C with 5% CO_2. After 2 h incubation, the tested samples were removed. In neutral red uptake (NRU) assay, treated Caco-2 cells were rinsed with PBS and then incubated for 3 h at 37 °C with 100 μL of cell culture medium containing 10% Neutral Red solution. After incubation, medium was removed and cells rinsed twice with Dulbecco's PBS before adding Neutral Red Assay solution. Plate was shaken 45 min at room temperature, and absorbance recorded at 540 nm with Synergy 4 microplate reader (BioTek Instruments, Inc., Winooski, USA). Before performing NRU assay, 50 μL of cell culture media were transferred into a new 96-well plate, mixed with 50 μL of working reagent for LDH detection and incubated for 20 min at room temperature in the dark. Reaction was blocked by adding 25 μL of the stop solution, and the amount of produced formazan was measured recording absorbance at 500 nm with Synergy 4 microplate reader. The assays were repeated three times independently, each run as three independent technical replicates. Results are reported as a percentage of control (treated with cell culture medium only) and expressed as mean ± standard deviation. The cytotoxicity of the PARG polymer solution was evaluated by NRU assay following the same protocol. The tested concentrations were 0.009, 0.017, 0.034, 0.068, 0.137, 0.205, and 0.274 mg/mL, which were equal to the amounts of PARG polymer involved in the tested PARG NCs concentration successively.

2.9. Measurement of the transepithelial resistance (TEER) and insulin transport across the Caco-2 monolayer

Caco-2 cell monolayers were cultured on tissue-cultured-treated PET filters (1 μm diameter, 1.1 cm^2, Millipore Transwell® 12 well/plate), and were used for experiments 21 days after seeding. The evaluation of PARG NCs was performed in Caco-2 cell monolayers for two NC concentrations: 0.5 mg/mL and 1 mg/mL. The cell culture medium and

the solutions containing the same amount of PARG and insulin were used as controls. The variation in the TEER values for the cell monolayer integrity assessment was measured with a Millicell-Electrical Resistance System (Endohm-12, Millipore Corp). Monolayers with a TEER values in the range of 800–1500 Ω cm^2 were used. Simultaneously, samples were collected (500 μL) from the receiver compartment and the apical compartment 2 h after NC cell monolayer exposure and the insulin concentrations were measured using a liquid chromatography - mass spectrometry. Cell monolayers were gently washed with NaCl 0.9% and frozen at −80 °C for insulin quantification within the cells. Liquid chromatography (Shimadzu HPLC system LC 20AD, Japan) with a 150 × 2.1 mm – 5 μm – 300 Å HPLC C8 column (Interchim, France) was used for the elution of insulin with a gradient method. The mobile phases A and B were 0.1% formic acid solution and acetonitrile containing 0.1% formic acid, respectively. The flow rate was 0.6 mL/min to avoid pressure rise. 100 μL of the tested sample was treated with 200 μL of chloroform/methanol/water at 1/1/0.3 and 100 μL of 0.1 M NaOH, and then 40 μL of analyte was injected onto the column placed in an oven at 60 °C. The total run time was 13 min. Tandem mass spectrometry (Quantum ultra) in positive electrospray mode was used for detection. System control and data processing were carried out using MassLynx software version 4.1. Spray voltage was 3.0 kV, and sheath and auxiliary gas pressures were 50 and 15 (arbitrary units), respectively. The in-source CID energy was fixed at 12 V, and capillary temperature was 350 °C. Tube lens and collision energy values were optimized for insulin. Multiple reaction monitoring was used for the detection of the ion transitions. The multiple reaction monitoring transitions for analytes was as follows: *m/z* insulin 709.805 > 731.76, *m/z* insulin 1284.73 > 1104.60. Analytes were quantified by means of calibration curves using insulin as internal standard. The standard curves showed linearity for creatine over a range of 0.025–10 μg mL^{-1} for insulin. The methodology for this assay involves reduction with dithiolthreitol 45 mM and alkylation with 100 mM of iodoacetamide 100 mM of intact insulin for measurement of the free B chain.

2.10. In vivo fluorescence imaging of DiD-loaded PARG NCs

One week before the experiment, the BALB/c mice were placed on a low manganese diet to reduce autofluorescence. The abdominal fur was removed by depilation. Prior to the experiment, the animals were fasted for 24 h, and then 200 μL of DiD loaded PARG NCs (NC 22 mg/mL, DiD 10 μg/mL, n = 4) or free DiD solution at the same concentration were administered to mice by oral gavage (n = 2). *In vivo* biodistribution was performed by total body scanning at different time points (0, 1, 3, 6, 24 h) on isoflurane/oxygen anesthetized animals, using a MX2 scanner (ART, Montreal, Canada). Confocal microscopy was used to further examine the interaction of PARG NCs with the intestinal epithelium. In control group, the mice were treated with free DiD instead of DiD-loaded PARG NCs. The intestines were dissected after treatment, washed with PBS and fixed in 4% PFA for 3 to 4 h at 4 °C. Afterwards, they were treated and stored at −80 °C for cryostate processing. Samples were then cut into 10 μm thick cryoslices using a Leica CM 1850 CM cryostat and transferred to slides (SuperFrost Plus, Thermo Scientific). Confocal images were acquired with Leica TCS SP5 II microscope and further processed using ImageJ software.

2.11. In vivo bioactivity of encapsulated insulin

All animal experiments were reviewed and approved by the ethics committee of the University of Santiago de Compostela (procedures from Prof. Carlos Diéguez, 1500AE/12 / FUN01/FIS02/CDG3) according to the European and Spanish regulations for the use of animals in animal studies; performed therefore in compliance with the Directive 2010/63/EU of the European Parliament and Council of 22nd September 2010 on the protection of animals used for scientific purposes; Spain Royal Decree 1201/2005, of October 10th, on the protection of animals used for experimental and other scientific purposes and under the Royal Decree 296/2008 of Spain 30th December on the protection of animals used for experimental and other scientific purposes, including teaching. Male Sprague-Dawley rats (247–272 g) were obtained from the Central Animals House of the University of Santiago de Compostela (Spain). The animals were fasted for 4 h prior to the experiments, with free access to water, and kept conscious for the duration of the experiment. Only those with initial glucose level over 65 mg/dL were selected for the study. A dose of insulin loaded PARG NCs (1 IU/kg) in a volume to weight ratio of 1 μL: 1 g rat was administered subcutaneously. As control, plain insulin solution was administered to the animals following the same procedure at the same dosage. Blood samples were collected from the tail vein 30 min prior to the subcutaneous administration to establish the baseline blood glucose level. At time point of 0.5, 1, 1.5, 2, 3, 4, 5, 6, 7, and 8 h after administration, blood samples were collected to monitor the glucose level change following the PARG NCs or insulin administration. The glucose level was measured using a glucometer (Glucocard™ G + meter, Arkray Factory, Japan).

2.12. In vivo efficacy studies in non-diabetic rats

For the *in vivo* evaluation of the hypoglycemic response, Male Sprague-Dawley rats (240–290 g) were obtained from the Central Animals House of the University of Santiago de Compostela (Spain). The animals were fasted for 4 h prior to the experiments, with free access to water, and kept conscious for the duration of the experiment. Only those with initial glucose level over 65 mg/dL were selected for the study. PARG NCs were administered intraduodenally (with or without 3% sodium glycocholate, SGC, in NC suspension) at an insulin dosage of 50 IU/kg body weight in a volume to weight ratio of 1 μL: 1 g rat, through a cannula inserted by surgery 1 week before the experiment. The animals used as control were administered blank PARG NCs without insulin loading, following the same procedure. Additionally, an insulin solution in saline was subcutaneously injected at a dose of 1 IU/kg in a volume to weight ratio of 1 μL: 1 g rat to a different group. Blood samples were collected from the tail vein 30 min prior to the oral administration in order to establish the baseline blood glucose level. At time point of 0.5, 1, 1.5, 2, 3, 4, 5, 6, 7, and 8 h after dosing, the blood samples were collected to monitor the glucose level change following the PARG NC or insulin administration. The glucose level was measured with a glucometer. For the control study and to test the mixability of PARG NCs and SIF, the purified and highly concentrated NCs were resuspended in water or sodium glycocholate (SGC) solution to 3% (w/v) SGC in the final formulation. Both were transferred to a glass vial that contained SIF, at a NC to SIF volume ratio proportional to the *in vivo* efficacy study condition with fasted state rats (~300 μL formulation in 3.2 mL SIF).

3. Results and discussion

The main objective of this work was to design, develop and characterize a peptide nanocarrier with a potential to confront all the barriers associated to the oral modality of administration. Because of our experience and the positive results we had obtained with chitosan NCs [13,14], we decided to adopt and optimize this NCs technology in order to obtain a NC prototype that could fulfill the requirements associated to the oral administration. As indicated in the introduction, the tailored properties were: i) capacity to load and control the release of the associated peptide; ii) stability in the intestinal fluids; iii) capacity to diffuse across the mucus layer; iv) capacity to interact with the intestinal epithelium and facilitate the transport of the associated peptide.

3.1. Physicochemical characteristics of NCs and association efficiency of insulin

A schematic representation highlighting the components and the organization within the NCs is shown in Fig. 1. These components and their appropriate concentrations were selected upon a thoughtful screening, as illustrated in Fig. 2. First, we explored the utility of two different oils, oleic acid and Miglyol® 812N, the last one being the most commonly used to formulate NCs [14,15,30–33], and fixed the rest of the formulation parameters: 0.4% (w/v) surfactant Labrasol®, and 0.1% (w/v) PARG. According to our results, the size of the particles and their polydispersity were smaller when using oleic acid instead of Miglyol® 812 N (233 nm *vs.* 310 nm; PDI 0.14 *vs.* 0.39 for oleic acid and Miglyol®). This size reduction of the formulation could be due to the chemical architecture of each oil matrix (C18 *vs.* C8/C10 triglycerides) and also to the higher viscosity of the oleic acid in comparison with Miglyol® 812N [34–36]. Based on this and also on its penetration enhancing properties [37,38], oleic acid was selected as a critical component of the NCs for further optimization.

In the second optimization stage, we analyzed simultaneously the effect of three different surfactants (Span® 80, Tween® 80 and Labrasol®) and PARG concentration on the physicochemical properties of the resulting nanocapsules. The results, shown in Fig. 3, indicate that the nanoemulsions prepared with the three surfactants have a negative charge ranging from −40 to −70 mV and a size of 200–300 nm. While Span® 80 and Labrasol® displayed similar *Z*-potential, around −70 mV (see Fig. 3), incorporation of Tween® 80 to the formulation led to a clear reduction of the superficial charge of the nanoemulsion (around −40 mV, see Fig. 3). Considering the molecular structure of these three surfactants (see Fig. 4), Tween® 80, with clearly differentiated hydrophobic/PEG domains can incorporate its hydrophobic moiety into the oil phase and extend its PEG arms towards the aqueous phase. This result in the displacement of the nanoemulsion slippery plane and then, in a reduction of the *Z*-potential magnitude [39]. However, upon addition of PARG to the NCs fabrication process, significant changes in size and zeta potential were observed. First, the nanosystems containing Span® 80 and Labrasol® exhibited an inversion of Z-potential from highly negative to positive, which should be attributed to the attachment of PARG, and hence to the formation of the NCs. This efficient attachment was only observed for concentrations of PARG of 1–2 mg/mL, whereas a lower concentration (0.5 mg/mL) only led to the destabilization of the nanosystem (size in the μm range and Z-potential close to cero). In contrast, in the case of Tween® 80, no change in size and a minor inversion in the zeta potential were observed. Consequently, we concluded that both the type of surfactant and the concentration of PARG play a critical role in the formation of the nanocapsular structure.

These observations could be explained by the different structure of these three surfactants. Tween® 80 contains hydrophobic domains and hydrophilic PEG sections, while Span® 80 is more hydrophobic, exhibiting only –OH groups as hydrophilic entities. On the other hand, Labrasol® is a mixture of glycerides modified with -PEG-C8/10 moieties. Considering this, we could speculate that the PEG moieties of Tween® 80 would be projected towards the surface of the nanocapsules, thus, hampering the adsorption of the PARG molecules. In contrast, the absence of a PEG shell in Span® 80 and Labrasol®- containing prototypes might facilitate the incorporation of PARG onto the O/W interface. To illustrate this explanation, Fig. 4 includes the schematic representation of the arrangement or these three non-ionic surfactants on the O/W interface of the systems.

In the next step, SDC was employed as a co-surfactant. The characterization of the resulting prototype indicated that the size of the SDC-containing NCs was reduced and the zeta potential could be modulated from +12 mV to −30 mV, depending on the balance between PARG and SDC. Despite the encouraging properties of the composition described above, these NCs turned out to be unstable after a few days' storage. In order to enhance the colloidal stability during storage, we added poloxamer 188 as a PEGylated protective shell. This shield was also expected to, firstly, increase the stability of the NCs when interacting with intestinal lipids and enzymes [34], and secondly, facilitate the diffusion of the NCs across the mucus [40,41].

Following the above formulation optimization process, we selected the specific ingredients as illustrated in Fig. 1. This specific prototype exhibited a hydrodynamic mean size of around 200 nm, low PDI and a negative *Z*-potential (shown in Table 1). In TEM analysis, the NCs displayed a smaller size than the one calculated by DLS. This could be due to the shrinking of the NCs during the drying process. The images also showed that the NCs have a spherical shape (Fig. 5).

The insulin incorporation into these NCs was expected to depend on the electrostatic and hydrophobic interactions between this drug molecule and various NC components. Such interactions are obviously associated with the solubility and ionization of insulin, both related to its

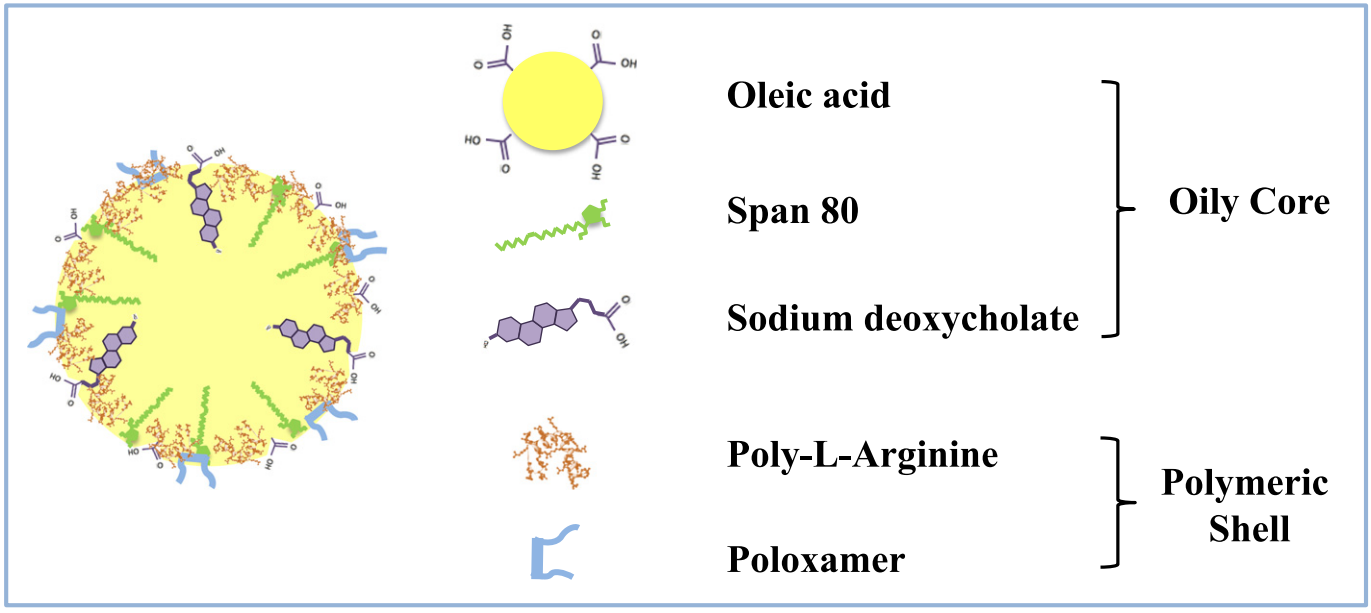

Fig. 1. Structural illustration of PARG NC and its components.

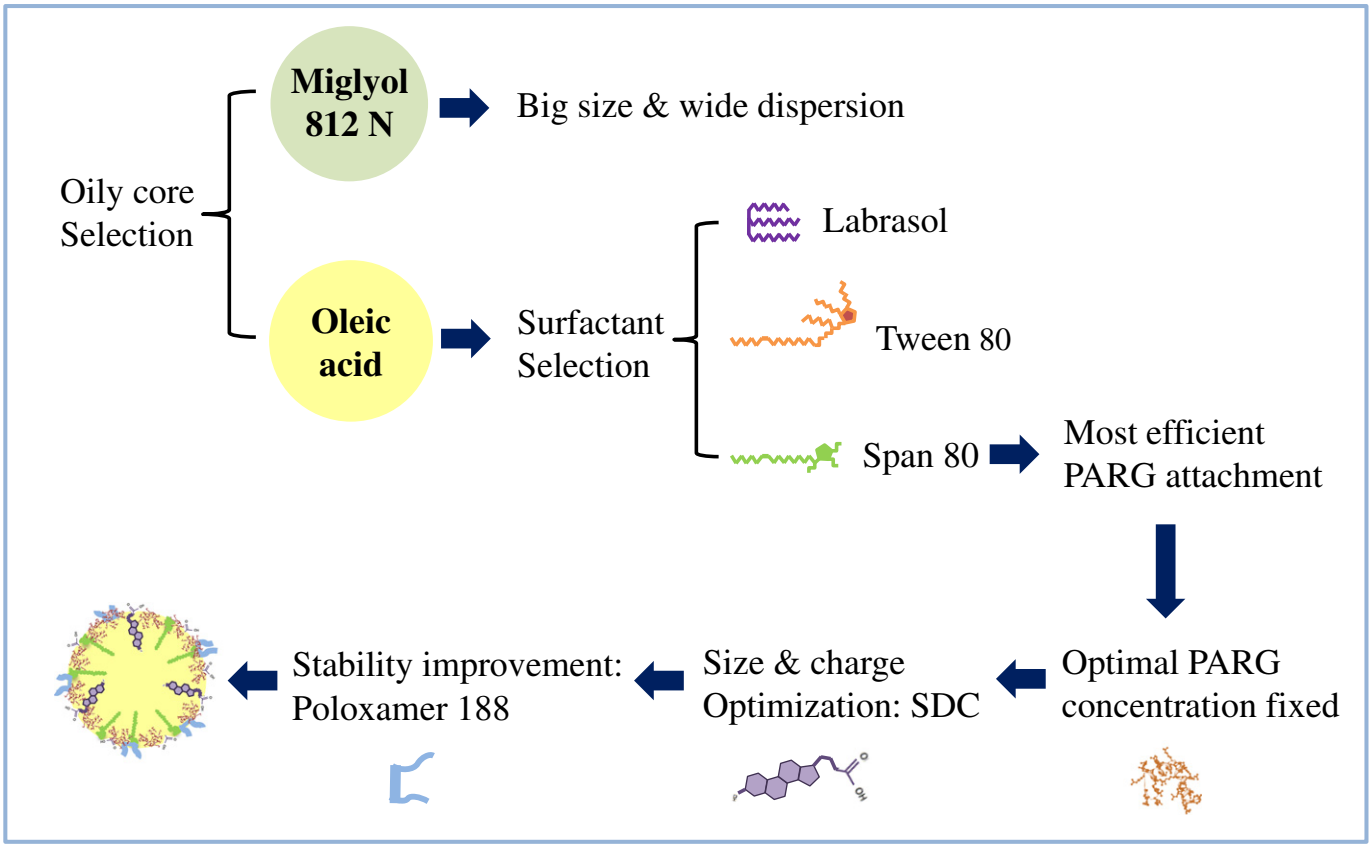

Fig. 2. Flow diagram that outlines the rational design process of PARG NCs.

isoelectric point (IP). In order to expose insulin molecules to different pH values, we adjusted the aqueous phase to different pH values which had an impact on the final pH of the formulations. As shown in Fig. 6, when the final pH of the formulation was close to the insulin IP (IP = 5.49), it was possible to reach an AE close to 80%. However, at pH values farther from this IP (either higher or lower), the insulin AE was clearly reduced. The increased on the insulin entrapped at the pH close to its IP could be attributed to the predominance of hydrophobic interaction between the hydrophobic domains of this peptide with the components of the NC core, and the reduced affinity of insulin towards the aqueous phase.

Given the importance of pH on the insulin encapsulation process, we explored the possibility of using a buffer as the aqueous phase in order to ensure a final formulation pH close to 5.4. Among the different buffer systems investigated, we found that the use of 20 mM acetate buffer led to the formation of NCs with a size of 185 ± 6 nm, a low PDI and an AE of 88 ± 5% (Table 1, determined by direct method and confirmed by indirect methods described in the methodology section). Taking into account that the production yield of the NCs is 74.21 ± 0.26% (w/w), the final insulin loading was 1.49% (w/w), a loading that was acceptable for subsequent studies.

3.2. Stability of PARG NCs in simulated biological media

We hypothesized that the success of the formulation would depend, at least in part, on its capacity to maintain its physicochemical properties under physiological conditions. Fig. 7 shows the particle size evolution of insulin loaded-PARG NCs in SIF (pH 6.8), FaSSIF-V2 (with bile salts, pH 6.5) and FeSSIF-V2 (with enzymes and bile salts, pH 5.8) media during 4 h. The results indicate that independent of the simulated intestinal media composition, the PARG NCs size (originally 178 nm) remained quite stable during the incubation time. Accordingly, the

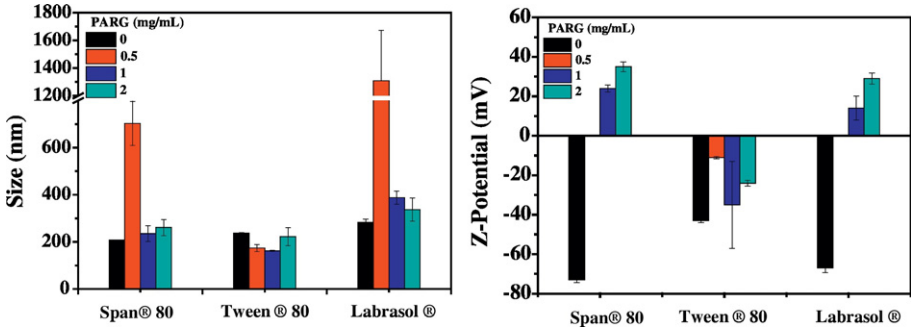

Fig. 3. Influence of surfactant type and PARG concentration on the physicochemical properties of blank formulations. When PARG concentration is 0, the system is a nanoemulsion. Mean ± S.D., n = 3.

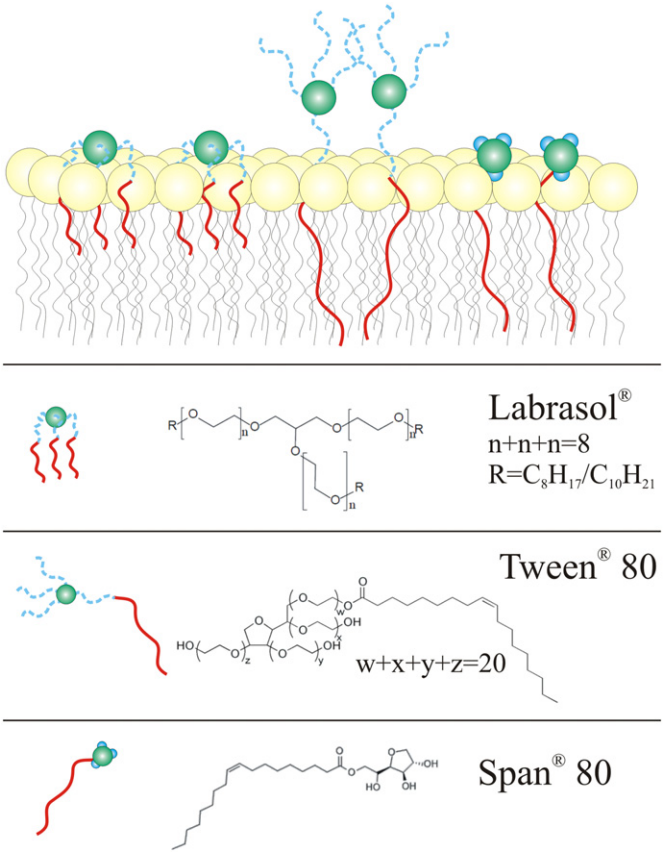

Fig. 4. Chemical structure and schematic representation of the arrangement of Span® 80, Tween® 80 and Labrasol®, in the O/W interface of the nanostructure. Red lines represent the hydrophobic moieties, while blue represent the hydrophilic fragments (dashed lines for PEG and spheres for –OH groups). Green spheres represent the linkers of each molecule.

count rate, providing an indication of the particle number in suspension, was hardly altered during the experiment [42]. This stability in biologically relevant media containing enzymes and bile salts has been attributed to the adequate protection of both the shell and our rational design [34]. A small decrease in particle size was observed upon dilution of the NCs in FeSSIF-V2, which could be attributed to the interference of the FeSSIF-V2 medium with the size measurement technique.

3.3. Colloidal stability of insulin-loaded PARG NCs during storage

Insulin-loaded PARG NCs were stored, as a suspension, at room temperature (~25 °C). The particle size and count rate were monitored up to 45 days (supporting materials Fig. S1), and the results showed that these PARG NCs remained stable over this period of time. In addition, insulin content in these NCs was determined at 0, 1, 3, and 15 days, and the insulin remaining unmodified. These positive preliminary stability data are in good agreement with the stabilization strategy defined in the formulation process of NCs.

3.4. In vitro release of insulin from PARG NCs

The release of insulin from PARG NCs was studied in different simulated intestinal media, *e.g.* in SIF and FaSSIF-V2 (SIF plus bile salts), which mimic the fasted state of the animals in the *in vivo* assay. The results obtained in SIF medium showed a negligible peptide release (data not shown). In contrast, in FaSSIF-V2 medium, 21% peptide release was evidenced at time 0 h, followed by a continuous release of up to 54% at 4 h (Fig. 8). The rest of insulin could be recovered from the NCs, upon their digestion. The 21% burst release was likely due to the immediate release of insulin molecules located near the surface of the nanocapsules. This profile also suggests that the presence of bile salts and surfactants in FaSSIF-V2 release medium triggered the release of insulin. Because the NCs were stable in this medium in terms of size (Section 3.2), we hypothesize that the bile salts and surfactants could be responsible for the disassociation of insulin exposed to the surface in the PARG/surfactants shell [43–45]. This sustained release profile is supposed to be of interest for the intestinal delivery of insulin. Indeed, the NCs are supposed to reach the intestinal epithelium in the duodenum-jejunum segments in the first hours upon oral administration. Once there, the NCs would provide a continuous delivery of the associated insulin. Eventually, after a few hours, the NCs would disintegrate and release their content.

3.5. Toxicity of PARG NCs on Caco-2 cells

The cytotoxicity of insulin loaded PARG NCs was evaluated in the Caco-2 model using the LDH and NRU assays. The results of the DHL assay shown in Fig. 9A, indicate that PARG NCs induced a dose-dependent toxicity after a 2 h incubation. LDH release from the damaged cells was observed when the concentration of NCs tested was 1.48 mg/mL or higher. Very similar results were observed when using the NRU assay (Fig. 9B). In this case, the cytotoxicity of PARG NCs was compared with that of the control nanoemulsion (same constituents as the NCs except PARG). The conclusion from these data was that the toxicity of the NC and NE was very similar, showing a significant toxicity only at the concentration of 1.48 mg/mL. On the other hand, the results shown in Fig. 9C indicate that the toxicity of the free PARG polymer was superior to that of the NCs and nanoemulsions. However, considering the limited amount of PARG polymer involved in NCs (0.03 mg/mL in each 0.74 mg/mL NCs), the conclusion was that PARG does not contribute significantly to the toxicity of the NCs. Overall, the toxicity profile observed for PARG NCs is similar to the one observed for similar compositions [17] and could be attributed, mainly, to the penetration enhancing effect of the NC components when interacting with the enterocytes [38,46].

3.6. Effect on the transepithelial electrical resistance (TEER)

Some cationic polymers, among them chitosan [13,47], are well-known for their capacity to open the intercellular tight junctions (TJs), thereby altering the transepithelial resistance and facilitating the paracellular transport of hydrophilic drugs. Recent reports from our own group [17] and others [46] have also claimed this functionality for PARG. In this study, we evaluated the effect of PARG NCs on the TEER of the Caco-2 monolayer and used a PARG solution as control.

Table 1
Physicochemical properties of insulin-loaded PARG NCs and blank PARG NCs, showing influence of pH/salt content (acetate buffer) of the external aqueous phase (PARG solution) on insulin association efficiency. Mean ± S.D., n ≥ 3.

NC Formulation	pH (PARG solution)	pH (NCs suspension)	Size (nm)	PDI	*Z*-pot (mV)	AE (%)
Insulin-NCs	4.9	3–3.5	213 ± 27	0.1	−3 ± 4	<10
	10.8	5–6	178 ± 20	0.1	−30 ± 2	81 ± 6
	5.5 (buffer)	5.2–5.4	185 ± 6	0.2	−24 ± 3	88 ± 5
Blank NCs	10.8	5–6	189 ± 5	0.1	−33 ± 3	–
	5.5 (buffer)	5.2–5.4	177 ± 5	0.1	−23 ± 2	–

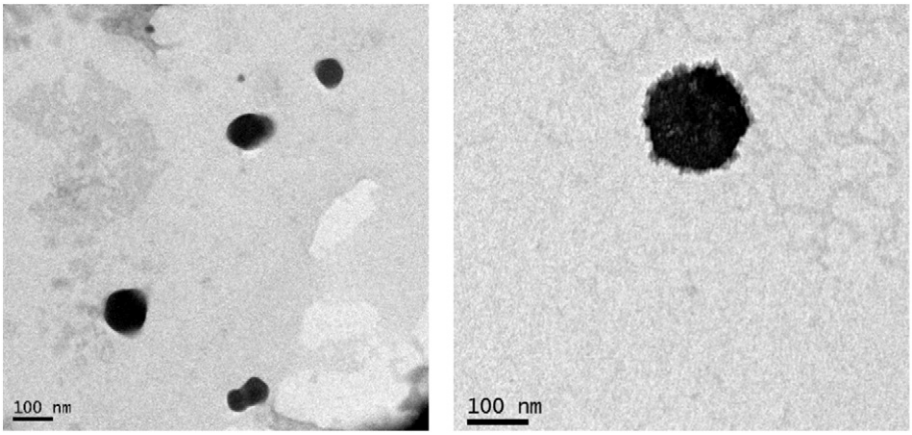

Fig. 5. Transmission electron micrographs of the PARG NC.

The results indicated that the TEER value of Caco-2 cells was not affected at a PARG NC concentration of 0.5 mg/mL (data not shown). However, consistent with our previous finding, when the concentration was increased up to 1 mg/mL, both PARG NCs and the free PARG induced a significant TEER decrease (15% and 38%, respectively) after a 2-h incubation period (Fig. 10). Interestingly, after removing PARG NCs, a significant TEER recovery was observed at 24 h, thus proving the transient opening of the TJs. In contrast, the TEER value was not recovered upon exposure to the free polymer. Overall, this study confirmed the capacity of PARG polymer to open the intercellular TJs [46], and showed that by incorporating this polymer to the PARG NC shell, it is possible to modulate the permeation enhancing capacity of the polymer. This may also suggest that the toxicity observed on the Caco-2 cells could be transitory.

3.7. Capacity of PARG NCs to enhance the transport of insulin

As shown in the previous section, PARG NCs are able to alter the TEER in a transient manner. In addition, in a previous study, we reported the capacity of PARG NCs with a different oil/surfactants composition to enter the Caco-2 monolayer [17]. Based on these results, our next objective was to analyze *in vitro* if the PARG formulation rationally designed in this study could work as an insulin carrier. The results shown in Fig. 11A and B indicate that, after a 2-h incubation period, 3.54 ± 0.27% of insulin associated to the NCs (1 mg/mL) had been transferred to the basolateral compartment and 1.29 ± 0.53% remained associated to the monolayer. In addition, a significant transport was also observed for the physical mixture of PARG and insulin (2.73 ± 0.32% transported and 0.67 ± 0.08%, retained in the cells) (Fig. 11A). In order to have an idea about the extent of this transport, we have compared these values with the only ones reported in the literature so far, which were obtained with chitosan-based nanoparticles, a nanocarrier extensively investigated for oral insulin administration [48]. According to this previous report, insulin associated to chitosan nanoparticles was transported up to ~1.3% across the Caco-2 monolayer within a 2 h time frame. Based on these data, we could conclude that the transport attained with PARG nanocapsules is superior than the one observed for chitosan nanoparticles. The interpretation of the positive data obtained for PARG NCs could be as follow. First, taking into account the transient changes in the TEER and the transport observed for insulin physically mixed with PARG, we could hypothesize that the paracellular pathway has contributed to the enhanced insulin transport. On the other hand, given that insulin penetration was higher for PARG nanocapsules than for the physical mixture PARG and insulin, we could speculate about the potential intracellular uptake of PARG nanocapsules. The higher insulin transport achieved with PARG NCs, when compared to free PARG, could be explained by the co-localization of the peptide in association with PARG and other permeation enhancers present in the formulation. In fact, the oleic acid and bile salts present in the NCs core are known to increase the fluidity of cell membrane, and enhance the membrane permeability [18,20,38,49,50].

3.8. In vivo fluorescence imaging of DiD-loaded PARG NCs

In order to have an *in vivo* preliminary estimation of the interaction of PARG NCs with the intestinal tract, we traced fluorescent DiD-labeled

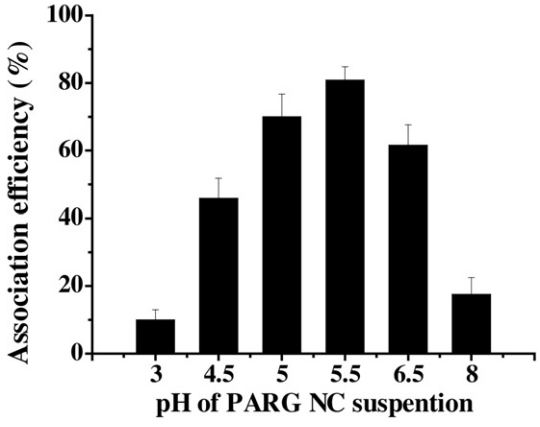

Fig. 6. Influence of pH of the PARG NC suspension on insulin association efficiency. Mean ± S.D., n = 3.

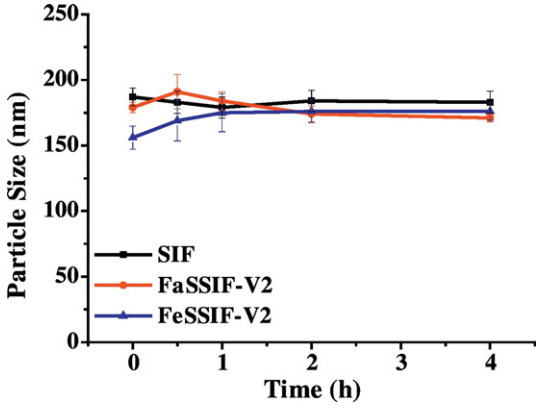

Fig. 7. Evolution of the particle size of PARG NCs upon incubation in SIF, FaSSIF-V2 and FeSSIF-V2 media at 37 °C. Attenuator of DLS fixed to 6. Mean ± S.D., n = 3. Original size of the formulation: 178 nm.

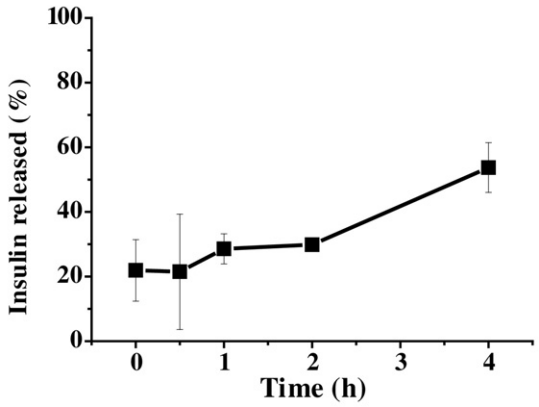

Fig. 8. *In vitro* insulin release profile of PARG NCs in FaSSIF-V2 medium. The amount of released insulin was calculated by determining the insulin amount remained associated to the NCs at the specific time points.

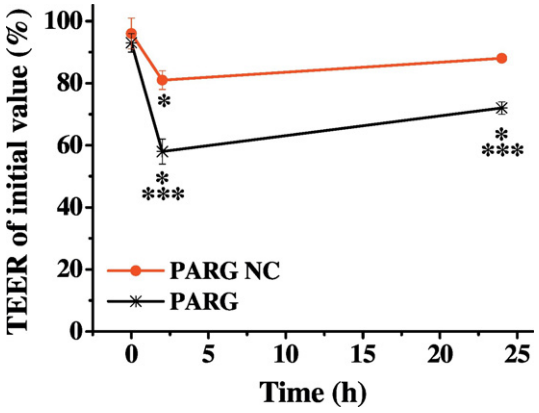

Fig. 10. TEER assay on Caco-2 cell monolayers exposed to PARG NCs (1 mg/mL, containing 0.045 mg/mL PARG and 0.014 mg/mL insulin) or to PARG polymer (0.045 mg/mL) + insulin (0.014 mg/mL). 2 h after exposure and 24 h after removal of the prototypes from the cells. Data expressed as mean ± SD, n = 3. Changes were considered statistically significant at $p < 0.05$: *$p < 0.05$ compared to non-treated control group; ***$p < 0.05$ compared to PARG NC group.

PARG NCs after oral administration to mice. The results obtained for representative rats are shown in Fig. 12. The bioluminescent image (Fig. 12A, acquired by the Optix Optiview™, ART, Montreal, Canada) shows the biodistribution of PARG NCs or free DiD dye following its administration by oral gavage to mice, and the histogram on (Fig. 12B) shows the mean of total photons emitted from the regions of interest (ROI, the rat body). The images suggest that both PARG NCs and free DiD dye are confined in the gastro-intestinal tract for up to 24 h. The association of free DiD to mucosa could be explained by the affinity of this amphiphilic dye to cell membrane. In fact, this dye is primarily used for labeling membranes. However, the analysis of florescence intensity gave some preliminary evidence of the greater retention of PARG NCs as compared to free dye.

A more detailed *in vivo* analysis involving dissection of the mice intestines (duodenum) at 1 h, 3 h, and 24 h after oral administration of

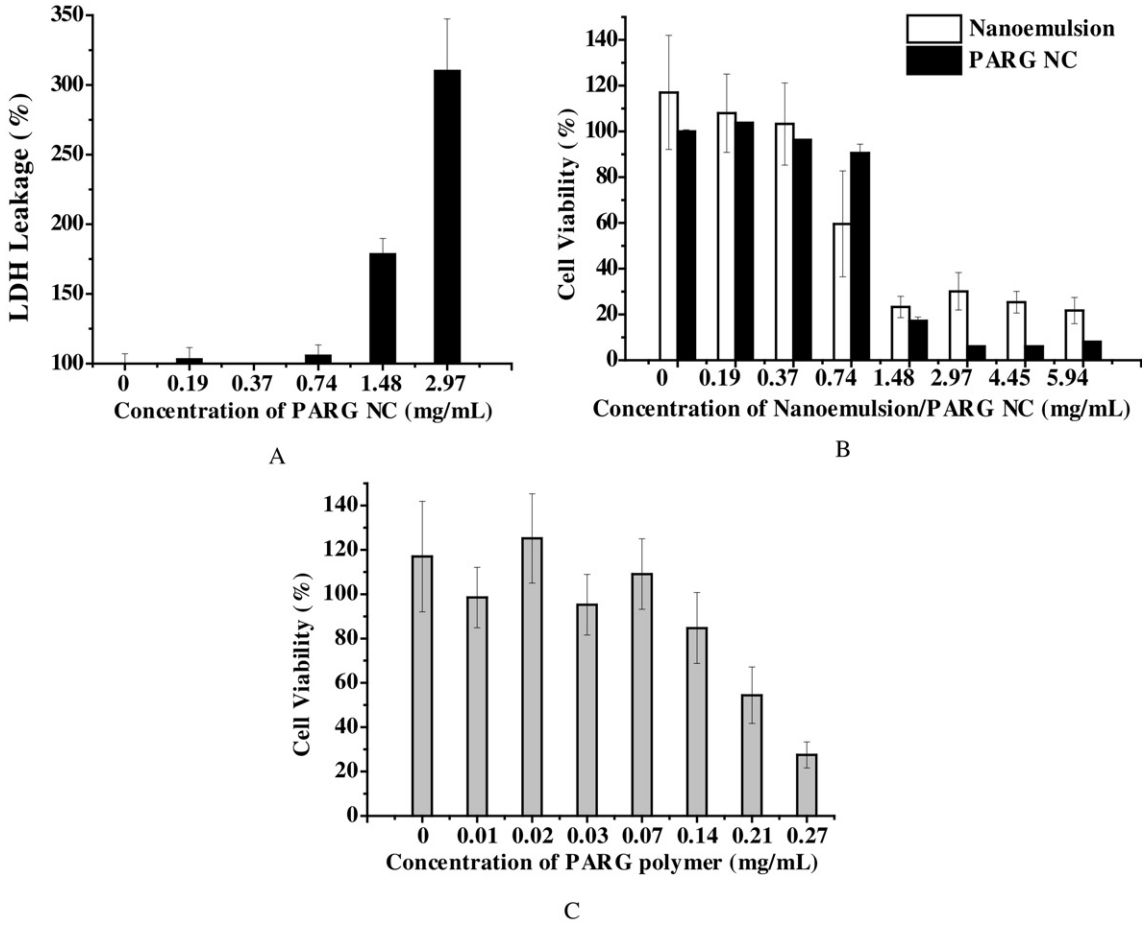

Fig. 9. Cytotoxicity of PARG NCs and the control groups (non-PARG coated nanoemulsion and PARG polymer solution) in Caco-2 cell line after 2 h incubation. (A) Cytotoxicity of PARG NCs determined by LDH assay; (B) Cytotoxicity of PARG NCs and control nanoemulsion determined by NRU assay; (C) Cytotoxicity of PARG polymers determined by NRU assay. Mean ± S.D., n = 3.

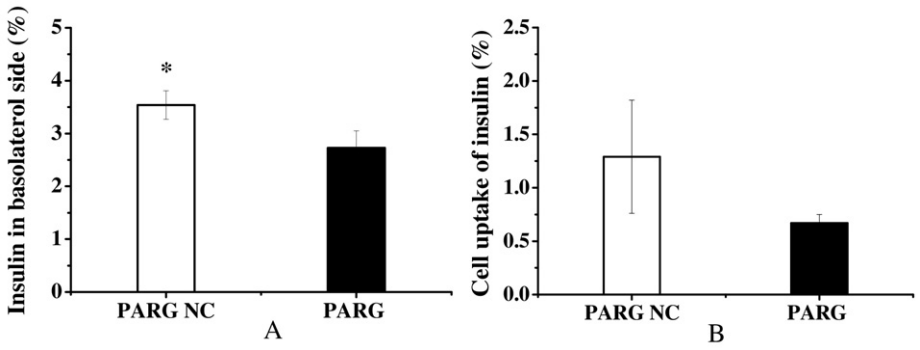

Fig. 11. Apical to basolateral transport of insulin across the Caco-2 cell monolayer under 37 °C, after 2 h incubation with insulin loaded PARG NCs (1 mg/mL, containing 0.045 mg/mL PARG and 0.014 mg/mL insulin) or PARG polymer (0.045 mg/mL) + insulin (0.014 mg/mL). Data expressed as mean ± SD, n = 3. Changes are considered statistically significant at $p < 0.05$, evaluated by ANOVA following Tuke's multiple comparison *post hoc* test (SigmaPlot SyStat Software Inc., San Joes, CA).

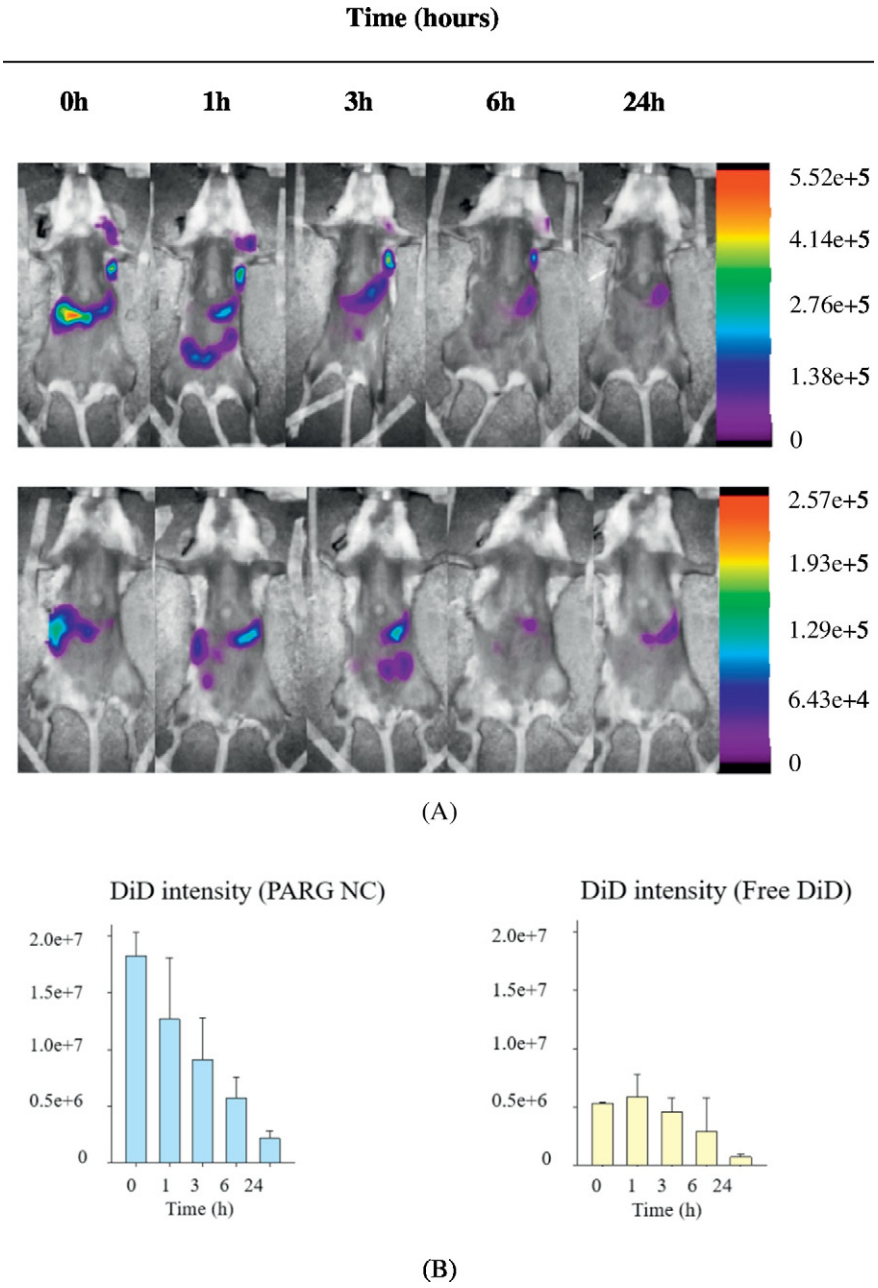

Fig. 12. (A) Fluorescence images of representative mice at 0, 1, 3, 6, and 24 h following oral administration of DiD labeled PARG NCs (up) and free DiD (down) dye and (B) the mean of total photons ± S.D. emitted from regions of interest around GIT. n = 4 for DiD-loaded PARG NC group, n = 2 for free DiD control group.

PARG NCs was performed. The results presented in Fig. 13 show an intense fluorescence signal overarching the duodenum villi 1 h after gavage. These images suggest that once PARG NCs reach the intestinal tract, they may diffuse through the mucus layer that covers the villi and reach the enterocytes. The fluorescence intensity observed within the duodenum region decreased significantly at 3 h after treatment, suggesting that the nanocapsules have moved away to lower intestinal regions (small and large intestine) or though the submucosal space. Despite the control experiments showing the absence of dye release from the NCs, we cannot discard the possibility that, under the *in vivo* conditions, the DiD dye could be released and diffuse through the body.

3.9. Bioactivity of encapsulated insulin and in vivo efficacy of PARG NCs

It is well known in the biotechnology field that the formulation process may result in the inactivation of labile macromolecules, such as peptides [51]. That is why; we thought it was important to analyze the bioactivity of peptides following their subcutaneous (s.c.) administration before studying the *in vivo* efficacy of the oral formulation. Thus, insulin-loaded PARG NCs were administered subcutaneously to fasted (4 h) healthy rats, using an insulin saline solution as control. The blood glucose level was normalized taking the 0 h mean glucose baseline value as 100%. As shown in Fig. 14, following the s.c. injection, both, the insulin solution and insulin-loaded NCs, exhibited a similar profile, where a drastic decrease in the glucose level was observed at 0.5 h and the normal levels were recovered at 3 h. From these results, it can be concluded that the mild conditions of the formulation process have not affected the bioactivity of the insulin.

Subsequently, an *in vivo* efficacy study was performed following intra-duodenal (50 IU/kg) administration to conscious healthy rats after 4 h fasting. Based on the results of a control experiment that showed that purified PARG NCs, highly deprived of surfactants, could have miscibility problems, the efficacy of PARG NCs was assessed in the absence or presence of SGC (3%, w/v). The colloidal stability of PARG NCs of the nanocapsuels was preserved in this medium and the dispersibility was greatly enhanced (Fig. 15).

The results show that the administration of insulin-loaded PARG NCs led to a significant decrease in the blood glucose levels, which lasted for less than two hours (Fig. 16). However, as expected, the co-administration of the NCs with SGC led to a prolongation of the hypoglycemic response (for up to 5 h). In addition to the well-known penetrating enhancing capacity of bile salts, the prolongation of the hypoglycemic response could be most probably associated to the improved dispersion of the formulation along the intestinal tract. Overall, as shown in Table 2, the apparent pharmacological bioavailability was 0.73% and 2.14% and the T_{max} extended from 1 h to 6 h, in the absence or presence of SGC.

Beyond the improved behavior of PARG NCs in the presence of SGC, the overall performance of the formulation must be considered modest. In principle, based on the rational design of the formulation and positive *in vitro* properties of same, notably, the observed preservation of the

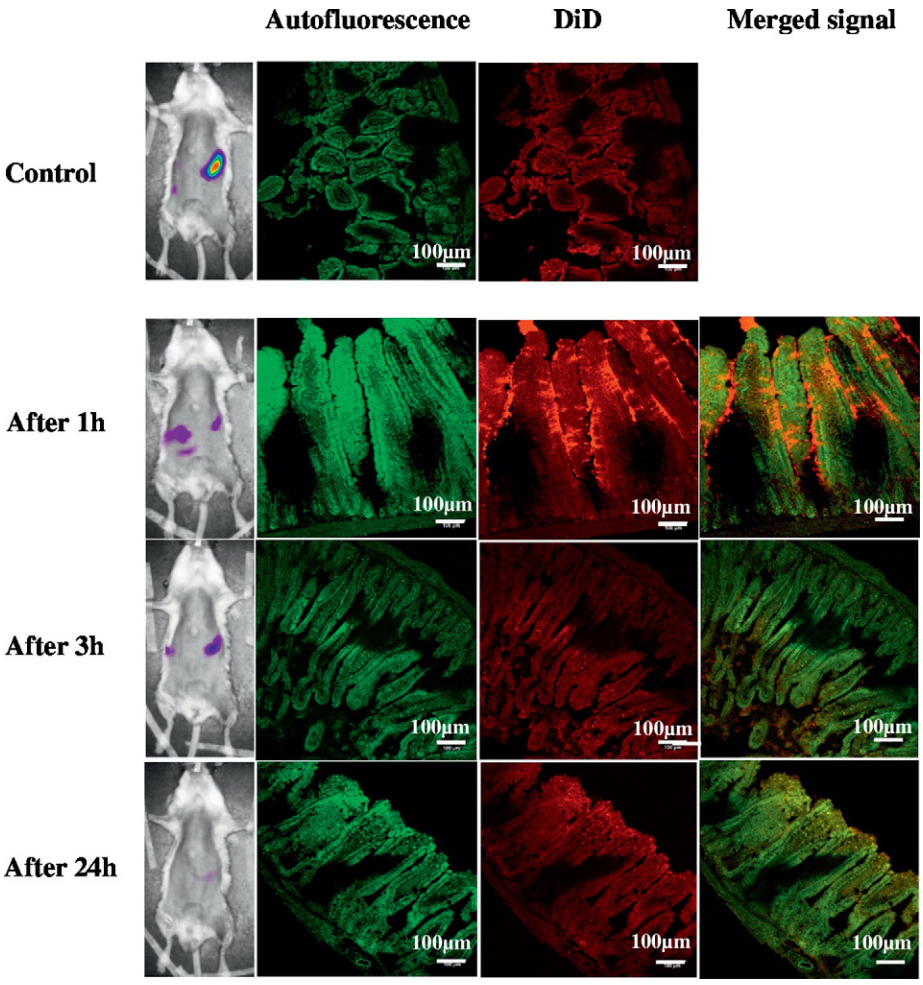

Fig. 13. Confocal images showing the interaction of DiD-loaded PARG NCs with mice duodenal tissue, 0 h, 1 h, 3 h, and 24 h after oral administration (20× magnification with air objectives).

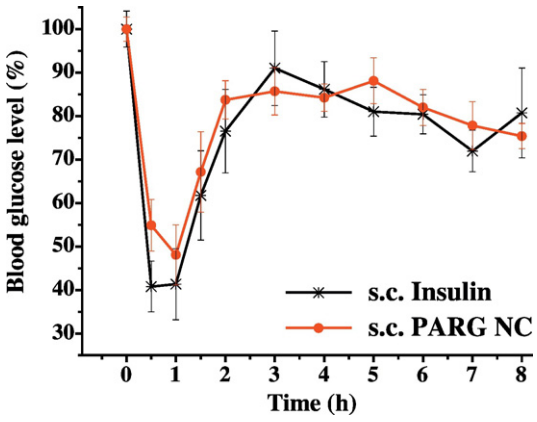

Fig. 14. Standardized hypoglycemic effect in healthy rats following subcutaneous administration of insulin-loaded PARG NCs and insulin saline solution at 1 IU/kg. Data represents the mean ± S.E., n = 8 for both groups.

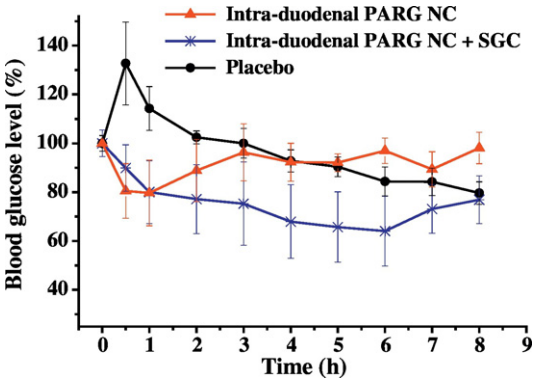

Fig. 16. Standardized hypoglycemic effect in healthy rats following intra-duodenal (with and without sodium glycocholate, SGC) administration of insulin-loaded PARG NCs at 50 IU/kg and blank PARG NCs as placebo. Data represents the mean ± S.E., n = 8 for insulin-loaded PARG NC groups and n = 7 for placebo.

insulin activity during the formulation process, the adequate stability in the intestinal media and the remarkable capacity of this formulation to promote the transport of insulin across a Caco-2 cells monolayer (Fig. 11), we expected a more significant response for this formulation. Our hypothesis to explain this modest efficacy is that, in the *in vivo* situation the NCs are highly diluted and, hence, their interaction with the epithelium maybe restricted. It is also possible that the *in vitro* assays and/or the *in vivo* experimental conditions used in the reported studies have a limited predictive value of the performance of these formulations. In this regard, it should be taken into account that, in agreement with our results, all the data reported so far using normoglycemic rats are very modest [30,52]. Most of the highly positive responses described until now have been achieved in diabetic rats or using anaesthetic drugs, which are known to alter the absorption process [53,54]. Indeed, when using the normal rat as model, the exogenous uptake of insulin may suppress the endogenous secretion of insulin by β-cells, leading to a milder hypoglycemic response [30]. On the contrary, the diabetic animals are over-sensitive to insulin because of the pancreas beta cell deficiency. In conclusion, the interpretation of these *in vivo* data should be evaluated cautiously, and larger animal models, *i.e.* pig model, will need to be taken into consideration for a subsequent assessment of the formulations we have developed.

From the studies performed so far, we conclude that the rational development of oral peptide delivery formulations and the translation of the *in vitro* data into the *in vivo* situation possess significant difficulties. However, we expect that the information reported here will help identify the critical steps to be considered in the design of such formulations. Further work on PARG formulations with the aim of incorporating the NCs in a final dosage form (enteric capsules) is expected to provide more elements to assess the performance of this new formulation.

4. Conclusion

In this work, we report the rational design of NCs consisting of an oily core made of penetration enhancers (oleic acid and SDC) and a polymer shell made of PARG, a polymer that is known for its ability to interact and increase the permeability of the cell membranes. The hypothesis behind this design was that the combination of lipids and penetration enhancers in the form of nanostructures would reinforce the capacity of the penetration enhancers to increase insulin transport. Our results clearly show that the NCs not only inherited the permeation enhancing properties of these biomaterials, but also allowed for a significant higher insulin transport across the Caco-2 monolayer when compared with the free PARG. *In vivo* studies indicated that PARG NCs could facilitate the interaction of both the peptide and the penetration enhancers with the intestinal epithelium, resulting in an overall increase on the peptide absorption. Further studies in large animal models will help assessing the value of this technology for oral peptide delivery.

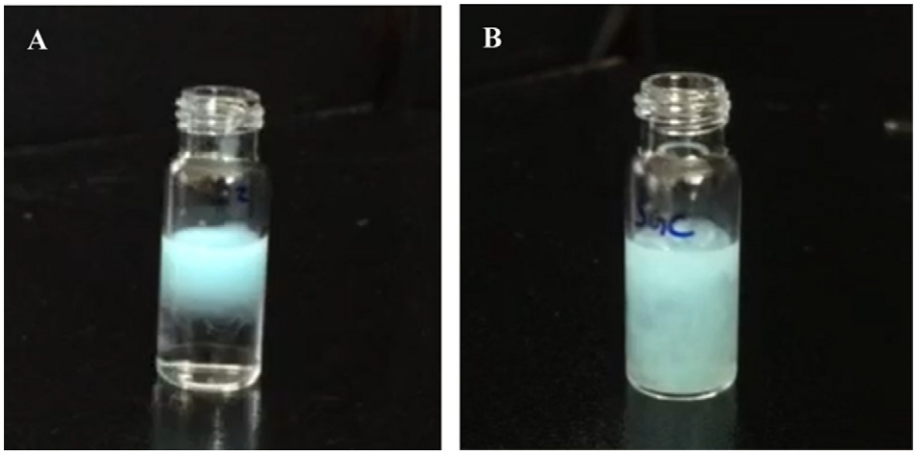

Fig. 15. Dispersibility of DiD-loaded blank PARG NCs in SIF (A) without and (B) with 3% (w/v) sodium glycocholate (SGC) in the NCs suspension medium. Photos were taken 1 min after mixing NCs and SIF without shaking.

Table 2
Parameters for plasma glucose levels and relative pharmacological bioavailability of insulin-loaded PARG NCs as compared to subcutaneously injected free insulin solution. Data expressed as mean ± S.E., n = 8 for all the groups except for intra-duodenally administrated PARG NCs with SGC (n = 7).

Formulations	Dose (IU/kg)	C_{min} (%)	T_{min} (h)	AAC	PA (%)
s.c. Insulin	1	41 ± 5.8	0.5	194.7	100
s.c. NCs	1	48 ± 6.9	1	171.6	88.2
Intra-duodenal NCs	50	80 ± 13.4	1	70.9	0.73
Intra-duodenal NCs with 3% SGC	50	64 ± 14.3	6	208.4	2.14

C_{min}: minimum plasma glucose concentration (% of initial), T_{min}: time to C_{min}.
AAC: area above the plasma glucose level time curves.
PA: relative pharmacological bioavailability, based on AAC for s.c. administration.

Acknowledgements

This work was supported by the European TRANS-INT Consortium, which received funding from the European Union's Seventh Framework Programme for research, technological development and demonstration under grant agreement No. 281035. Z. Niu also would like to thank the Chinese Scholarship Council for his scholarship.

Appendix A. Supplementary data

Supplementary data to this article can be found online at http://dx.doi.org/10.1016/j.jconrel.2017.02.024.

References

[1] K. Fosgerau, T. Hoffmann, Peptide therapeutics: current status and future directions, Drug Discov. Today 20 (2015) 122–128.
[2] T.A.S. Aguirre, D. Teijeiro-Osorio, M. Rosa, I.S. Coulter, M.J. Alonso, D.J. Brayden, Current status of selected oral peptide technologies in advanced preclinical development and in clinical trials, Adv. Drug Deliv. Rev. (2016) (In press).
[3] M. Garcia-Fuentes, M.J. Alonso, Chitosan-based drug nanocarriers: where do we stand? J. Control. Release 161 (2012) 496–504.
[4] M. Morishita, N.A. Peppas, Is the oral route possible for peptide and protein drug delivery? Drug Discov. Today 11 (2006) 905–910.
[5] M.R. Rekha, C.P. Sharma, Oral delivery of therapeutic protein/peptide for diabetes—future perspectives, Int. J. Pharm. 440 (2013) 48–62.
[6] B. Griffin, C. O'Driscoll, Opportunities and challenges for oral delivery of hydrophobic versus hydrophilic peptide and protein-like drugs using lipid-based technologies, Ther. Deliv. 2 (2011) 1633–1653.
[7] Z. Niu, I. Conejos-Sánchez, B.T. Griffin, C.M. O'Driscoll, M.J. Ajlonso, Lipid-based nanocarriers for oral peptide delivery, Adv. Drug Deliv. Rev. (2016) (In press).
[8] A. Beloqui, A. des Rieux, V. Préat, Mechanisms of transport of polymeric and lipidic nanoparticles across the intestinal barrier, Adv. Drug Deliv. Rev. (2016) (In press).
[9] S. Sherwyn, G. Blair, R. Len, L. John, A Two-week Randomized Active Comparator Study of Two HDV-insulin Routes (SC and Oral) and SC Human Insulin in Patients With Type 1 Diabetes Mellitus, 2015.
[10] J. Li, Y. Wang, L. Han, X. Sun, H. Yu, Y. Yu, Time–action profile of an oral enteric insulin formulation in healthy Chinese volunteers, Clin. Ther. 34 (2012) 2333–2338.
[11] A. Vol, O. Gribova, Methods and compositions for oral administration of protein and peptide therapeutic agents, in, Google Patents, 2010.
[12] C. Prego, M. García, D. Torres, M.J. Alonso, Transmucosal macromolecular drug delivery, J. Control. Release 101 (2005) 151–162.
[13] C. Prego, M. Fabre, D. Torres, M. Alonso, Efficacy and mechanism of action of chitosan nanocapsules for oral peptide delivery, Pharm. Res. 23 (2006) 549–556.
[14] C. Prego, D. Torres, M.J. Alonso, Chitosan nanocapsules as carriers for oral peptide delivery: effect of chitosan molecular weight and type of salt on the in vitro behaviour and in vivo effectiveness, J. Nanosci. Nanotechnol. 6 (2006) 2921–2928.
[15] C. Prego, D. Torres, E. Fernandez-Megia, R. Novoa-Carballal, E. Quinoa, M.J. Alonso, Chitosan-PEG nanocapsules as new carriers for oral peptide delivery. Effect of chitosan pegylation degree, J. Control. Release 111 (2006) 299–308.
[16] M.V. Lozano, G. Lollo, M. Alonso-Nocelo, J. Brea, A. Vidal, D. Torres, M.J. Alonso, Polyarginine nanocapsules: a new platform for intracellular drug delivery, J. Nanoparticle Res. 15 (2013).
[17] G. Lollo, A. Gonzalez-Paredes, M. Garcia-Fuentes, P. Calvo, D. Torres, M.J. Alonso, Polyarginine nanocapsules as a potential oral peptide delivery carrier, J. Pharm. Sci. (2017) (In press).
[18] A. Suzuki, M. Morishita, M. Kajita, K. Takayama, K. Isowa, Y. Chiba, S. Tokiwa, T. Nagai, Enhanced colonic and rectal absorption of insulin using a multiple emulsion containing eicosapentaenoic acid and docosahexaenoic acid, J. Pharm. Sci. 87 (1998) 1196–1202.
[19] Y. Lo, J. Huang, effects of sodium deoxycholate and sodium caprate on the transport of epirubicin in human intestinal epithelial Caco-2 cell layers and everted gut sacs of rats, Biochem. Pharmacol. 59 (2000) 665–672.
[20] Y. Onuki, M. Morishita, K. Takayama, Formulation optimization of water-in-oil-water multiple emulsion for intestinal insulin delivery, J. Control. Release 97 (2004) 91–99.
[21] T.N. Engelbrecht, A. Schroeter, T. Hauss, R.H. Neubert, Lipophilic penetration enhancers and their impact to the bilayer structure of stratum corneum lipid model membranes: neutron diffraction studies based on the example oleic acid, Biochim. Biophys. Acta 1808 (2011) 2798–2806.
[22] M.J. Hackett, J.L. Zaro, W.C. Shen, P.C. Guley, M.J. Cho, Fatty acids as therapeutic auxiliaries for oral and parenteral formulations, Adv. Drug Deliv. Rev. 65 (2013) 1331–1339.
[23] R. Rastogi, S. Anand, V. Koul, Evaluation of pharmacological efficacy of 'insulin-surfoplex' encapsulated polymer vesicles, Int. J. Pharm. 373 (2009) 107–115.
[24] S. Sun, N. Liang, Y. Kawashima, D. Xia, F. Cui, Hydrophobic ion pairing of an insulin-sodium deoxycholate complex for oral delivery of insulin, Int. J. Nanomedicine 6 (2011) 3049–3056.
[25] M.J. Santander-Ortega, A.B. Jodar-Reyes, N. Csaba, D. Bastos-Gonzalez, J.L. Ortega-Vinuesa, Colloidal stability of pluronic F68-coated PLGA nanoparticles: a variety of stabilisation mechanisms, J. Colloid Interface Sci. 302 (2006) 522–529.
[26] P. Calvo, C. Remuñán-López, J.L. Vila-Jato, M.J. Alonso, Development of positively charged colloidal drug carriers: chitosan-coated polyester nanocapsules and submicron-emulsions, Colloid Polym. Sci. 275 (1997) 46–53.
[27] G. Lollo, G.R. Rivera-Rodriguez, J. Bejaud, T. Montier, C. Passirani, J.P. Benoit, M. Garcia-Fuentes, M.J. Alonso, D. Torres, Polyglutamic acid-PEG nanocapsules as long circulating carriers for the delivery of docetaxel, Eur. J. Pharm. Biopharm. 87 (2014) 47–54.
[28] E. Jantratid, N. Janssen, C. Reppas, J.B. Dressman, Dissolution media simulating conditions in the proximal human gastrointestinal tract: an update, Pharm. Res. 25 (2008) 1663–1676.
[29] E. Roger, F. Lagarce, J.P. Benoit, The gastrointestinal stability of lipid nanocapsules, Int. J. Pharm. 379 (2009) 260–265.
[30] C. Damgé, C. Michel, M. Aprahamian, P. Couvreur, New approach for oral administration of insulin with polyalkylcyanoacrylate nanocapsules as drug carrier, Diabetes 37 (1988) 246–251.
[31] C. Damgé, C. Michel, M. Aprahamian, P. Couvreur, J.P. Devissaguet, Nanocapsules as carriers for oral peptide delivery, J. Control. Release 13 (1990) 233–239.
[32] S. Watnasirichaikul, N. Davies, T. Rades, I. Tucker, Preparation of biodegradable insulin nanocapsules from biocompatible microemulsions, Pharm. Res. 17 (2000) 684–689.
[33] S. Watnasirichaikul, T. Rades, I.G. Tucker, N.M. Davies, Effects of formulation variables on characteristics of poly (ethylcyanoacrylate) nanocapsules prepared from w/o microemulsions, Int. J. Pharm. 235 (2002) 237–246.
[34] M. Plaza-Oliver, J.F. Baranda, V. Rodríguez Robledo, L. Castro-Vázquez, J. Gonzalez-Fuentes, P. Marcos, M.V. Lozano, M.J. Santander-Ortega, M.M. Arroyo-Jimenez, Design of the interface of edible nanoemulsions to modulate the bioaccessibility of neuroprotective antioxidants, Int. J. Pharm. 490 (2015) 209–218.
[35] D.S. Viswanath, T.K. Ghosh, D.H.L. Prasad, N.V.K. Dutt, K.Y. Rani, Viscosity of LiquidsTheory, Estimation, Experiment, and Data, Springer Science & Business Media, 2007.
[36] Surface and interfacial forces - from fundamentals to applications, Prog. Colloid Polym. Sci. (2008).
[37] M. Morishita, A. Matsuzawa, K. Takayama, K. Isowa, T. Nagai, Improving insulin enteral absorption using water-in-oil-in-water emulsion, Int. J. Pharm. 172 (1998) 189–198.
[38] L.Y. Wang, J.K. Ma, W.F. Pan, D. Toledo-Velasquez, C.J. Malanga, Y. Rojanasakul, Alveolar permeability enhancement by oleic acid and related fatty acids: evidence for a calcium-dependent mechanism, Pharm. Res. 11 (1994) 513–517.
[39] J.N. Israelachvili, Intermolecular and Surface Forces, Elsevier Science, 2011.
[40] L.M. Ensign, R. Cone, J. Hanes, Oral drug delivery with polymeric nanoparticles: the gastrointestinal mucus barriers, Adv. Drug Deliv. Rev. 64 (2012) 557–570.
[41] K. Maisel, L. Ensign, M. Reddy, R. Cone, J. Hanes, Effect of surface chemistry on nanoparticle interaction with gastrointestinal mucus and distribution in the gastrointestinal tract following oral and rectal administration in the mouse, J. Control. Release 197 (2015) 48–57.
[42] G. Bastiat, C.O. Pritz, C. Roider, F. Fouchet, E. Lignieres, A. Jesacher, R. Glueckert, M. Ritsch-Marte, A. Schrott-Fischer, P. Saulnier, J.P. Benoit, A new tool to ensure the fluorescent dye labeling stability of nanocarriers: a real challenge for fluorescence imaging, J. Control. Release 170 (2013) 334–342.
[43] J. Liu, T. Gong, C. Wang, Z. Zhong, Z. Zhang, Solid lipid nanoparticles loaded with insulin by sodium cholate-phosphatidylcholine-based mixed micelles: preparation and characterization, Int. J. Pharm. 340 (2007) 153–162.
[44] P.C. Christophersen, L. Zhang, M. Yang, H.M. Nielsen, A. Mullertz, H. Mu, Solid lipid particles for oral delivery of peptide and protein drugs I—elucidating the release mechanism of lysozyme during lipolysis, Eur. J. Pharm. Biopharm. 85 (2013) 473–480.
[45] M. Garcia-Fuentes, D. Torres, M.J. Alonso, New surface-modified lipid nanoparticles as delivery vehicles for salmon calcitonin, Int. J. Pharm. 296 (2005) 122–132.
[46] T. Yamaki, Y. Kamiya, K. Ohtake, M. Uchida, T. Seki, H. Ueda, J. Kobayashi, Y. Morimoto, H. Natsume, A mechanism enhancing macromolecule transport through paracellular spaces induced by poly-L-arginine: poly-L-arginine induces the internalization of tight junction proteins via clathrin-mediated endocytosis, Pharm. Res. 31 (2014) 2287–2296.
[47] C. Prego, D. Torres, M.J. Alonso, The potential of chitosan for the oral administration of peptides, Expert Opin. Drug Deliv. 2 (2005) 843–854.

[48] A.M.M. Sadeghi, F.A. Dorkoosh, M.R. Avadi, M. Weinhold, A. Bayat, F. Delie, R. Gurny, B. Larijani, M. Rafiee-Tehrani, H.E. Junginger, Permeation enhancer effect of chitosan and chitosan derivatives: comparison of formulations as soluble polymers and nanoparticulate systems on insulin absorption in Caco-2 cells, Eur. J. Pharm. Biopharm. 70 (2008) 270–278.
[49] L. Zhao, J. Ding, P. He, C. Xiao, Z. Tang, X. Zhuang, X. Chen, An efficient pH sensitive oral insulin delivery system enhanced by deoxycholic acid, J. Control. Release 152 (Suppl. 1) (2011) e184–e186.
[50] B.S. Ramakrishna, M. Mathan, V.I. Mathan, Alteration of colonic absorption by long-chain unsaturated fatty acids. Influence of hydroxylation and degree of unsaturation, Scand. J. Gastroenterol. 29 (1994) 54–58.
[51] M.C. Manning, G.J. Evans, R.W. Payne, Protein stability during bioprocessing, Formulation and Process Development Strategies for Manufacturing Biopharmaceuticals, Inc, John Wiley & Sons 2010, pp. 605–624.
[52] M. Morishita, T. Goto, K. Nakamura, A.M. Lowman, K. Takayama, N.A. Peppas, Novel oral insulin delivery systems based on complexation polymer hydrogels: single and multiple administration studies in type 1 and 2 diabetic rats, J. Control. Release 110 (2006) 587–594.
[53] N. Reix, A. Parat, E. Seyfritz, R. Van Der Werf, V. Epure, N. Ebel, L. Danicher, E. Marchioni, N. Jeandidier, M. Pinget, Y. Frère, S. Sigrist, In vitro uptake evaluation in Caco-2 cells and in vivo results in diabetic rats of insulin-loaded PLGA nanoparticles, Int. J. Pharm. 437 (2012) 213–220.
[54] M. Niu, Y. Lu, L. Hovgaard, P. Guan, Y. Tan, R. Lian, J. Qi, W. Wu, Hypoglycemic activity and oral bioavailability of insulin-loaded liposomes containing bile salts in rats: the effect of cholate type, particle size and administered dose, Eur. J. Pharm. Biopharm. 81 (2012) 265–272.